



Quantitative analysis of liquid crystal-based immunoassay using rectangular capillaries as sensing platform

JHIH-WEI HUANG,¹ HIDEAKI HISAMOTO,² AND CHIH-HSIN CHEN^{1,*}

¹Department of Chemistry, Tamkang University, New Taipei City 25137, Taiwan

²Graduate School of Engineering, Osaka Prefecture University, 1-1 Gakuen-cho, Nakaku, Sakai City, Osaka 599-8531, Japan

*chc@mail.tku.edu.tw

Abstract: In past studies, liquid crystal (LC)-based immunoassays were accomplished by fabricating an LC cell with two pieces of glass slides after immunobinding, which makes the determination of the immunoassay not in real-time and requires trained personnel. Herein, we developed the LC-based immunoassay by using rectangular capillaries as the substrate for immunobinding. The inner surface of rectangular capillaries was decorated with a long alkyl saline, dimethyloctadecyl[3-(trimethoxysilyl)propyl]ammonium chloride (DMOAP), followed by immobilization of human serum albumin (HSA) as the probe. In this situation, the orientation of LC was homeotropic and dark LC image was observed under polarized light. When the solution containing anti-human serum albumin (anti-HSA) were dispensed into the capillary through capillary action, the specific immunobinding between HSA and anti-HSA formed an immunocomplex on the inner surface of capillary, which disrupted the original orientation of LC and led to a dark-to-bright transition of the LC images. The quantification of anti-HSA can be achieved by measuring the length of the bright LC image in the rectangular capillary. By using this immunoassay, the limit of detection (LOD) for anti-HSA is 1 $\mu\text{g/mL}$, and it did not respond to HSA and anti-human immunoglobulin G (anti-h-IgG). On the other hand, the diversity of the LC-based immunoassay can be extended for HSA detection when we immobilized anti-HSA in the capillary. Because the post-fabrication of LC cell was waived by using rectangular capillaries to develop the LC-based immunoassay, it is more convenient for users to handle and collect more reliable data. Moreover, the results of the immunoassay were visualized through naked-eye and could be recorded by a smartphone; it is more suitable for portable and point-of-care applications.

© 2019 Optical Society of America under the terms of the [OSA Open Access Publishing Agreement](#)

1. Introduction

In current biological and medical studies, protein detection is mostly accomplished by using immunoassays in which the proteins are chemically linked with different signal tags, e.g., enzymes [1–3], fluorescent molecules [4,5], electrochemically active molecules [6,7]. Upon the specific immunobinding between antigen-antibody pairs, the presence of the target proteins can be reported through the optical or electric signals produced by the tags. Currently, immunoassay technologies are well-developed and have been widely used in labs, clinics and hospitals. However, they suffered from some drawbacks such as complex pre-mixing and washing procedures, such that they have to be performed by trained personnel. Besides, because current immunoassays employ optical and electric signals, which require expensive instrumentation to collect quantitative data. Therefore, they are not affordable to general users. Based on these reasons, the extensive applications of immunoassay in daily life are limited.

In addition to the abovementioned immunoassays, the immunoassay can also apply liquid crystal (LC) as the signal reporters [8–11]. In between of two pieces of glass substrates where the LCs are aligned in the same orientation, the specific binding between antigen-antibody

occurred on the substrate alters the original orientation of LC. As a result, the optical images of LC under polarized light are changed. Based on this principle, LC-based immunoassays for detecting various antigens (e.g., HSA, CA-125) [8,9] and antibodies (e.g., anti-IgG, anti-hepatitis B) [10,11] have been developed previously. Because LC-based immunoassay shows colorful signals, its results can be easily understood by untrained personnel through naked-eye. This feature waives the cost of LC-based immunoassay from expensive instrumentation. The limit of detection (LOD) for protein detection could reach 1 $\mu\text{g}/\text{mL}$. However, the operation of current LC-based immunoassay requires labor-intensive procedures, such as substrate washing and cell fabrication that are subject to human errors. Moreover, the thickness of LC film in between of two pieces of glass substrates is affected by the quality of the spacer and the binder clips that is subject to batch-to-batch variations. Therefore, accuracy and reproducibility for LC-based immunoassays is still a problem when they are applied for routine disease diagnosis. Besides, because the LC-based immunoassays only provide on/off signals, the quantitative information of the assays is insufficient.

Rectangular (or square) capillaries are the glass materials with inner channel, which are commercially available with various dimensions. In past studies, rectangular capillaries had been widely adopted as the glass substrate to develop the system of capillary electrophoresis for separating a specific target from a mixture. In contrast, the researches on using rectangular capillaries for sensor applications are still in infancy. In past studies, Shirai et al. developed the fluorescence-based immunoassay for IgG detection by using a square glass capillary [12]. In their results, the reaction time required for immunocomplex formation in the capillary was significantly reduced (within 1 min) because of the minimized reaction scale, which demonstrated the advantage of using rectangular capillaries as the sensing platform of immunoassay. In terms of LC-based sensor, Khan et al. previously developed a method to determine glucose concentration in square capillary based on backscattering interferometry measurement of LC [13]. On the other hand, Kim et al. reported a method to report trypsin activity in round capillary based on the change in optical texture of LC [14]. Both results showed that LC can be applied as the optical signal reporter for the capillary-based sensing platform. Nevertheless, the quantification for the former required an expensive instrumentation, while the latter did not provide the quantitative data. To develop the immunoassays suitable for routine diagnoses, a simple and cost-effective quantification method is required.

Herein, we developed the LC-based immunoassay by using rectangular capillaries as the sensing platform for quantitative analysis of protein concentration for the first time. We immobilized human serum albumin (HSA) as the probe protein on the inner surface of capillaries. In the presence of anti-HSA, it is anticipated that the formation of immunocomplex on the surface would disrupt the original orientation of LC and result in the change in optical texture of LC that can be observed under polarized light. In contrast to previous LC-based immunoassay that applied two pieces of slides to fabricate the LC cell, the advantages by using rectangular capillaries to develop LC-based immunoassay could be: (1) the procedure of LC cell fabrication is waived such that operating procedure of the immunoassay is simplified which minimizes the effects from human errors; (2) the dimension of the LC in the capillary is fixed such that the reproducibility of the immunoassay is improved. In this work, we investigated how the immunobinding affects the LC texture in the rectangular capillaries and demonstrated how to use the length of optical signal in the rectangular capillary as the quantitative index for the LC-based immunoassay.

2. Materials and methods

2.1 Materials

Rectangular capillaries with inner dimensions of 0.1 mm (depth) \times 1 mm (width) \times 5 cm (length) were obtained from Super Chroma. *N,N*-Dimethyl-*n*-octadecyl-3-aminopropyltrimethoxysilyl chloride (DMOAP), HSA, anti-HSA, anti-IgG and Tween 20

were purchased from Sigma Aldrich. Polyethylenimine (PEI) was purchased from Fluka. Phosphate buffer saline (PBS) was purchased from UniRegion Bio-Tech, Taiwan. Liquid crystal 4-cyano-4'-pentylbiphenyl (5CB) and 4'-n-decyloxybiphenyl-4-carboxylic acid was purchased from TCI. Water was purified by using a Milli-Q system (Millipore).

2.2 Preparation of DMOAP-coated rectangular capillaries

To clean the inner surface, rectangular capillaries were immersed in a 5% Decon-90 solution (a commercially available detergent) for 2 h, sonicated in DI water for 15 min, and rinsed thoroughly with DI water twice. After this, the rectangular capillaries were dried under a stream of nitrogen. The cleaned rectangular capillaries were immersed in an aqueous solution containing 0.1% (v/v) DMOAP for 10 min, and then rinsed with copious amounts of DI water. DMOAP-coated rectangular capillaries were dried under a stream of nitrogen and heated in a 100°C vacuum oven for 15 min.

2.3 Preparation of HSA-immobilized and anti-HSA-immobilized rectangular capillaries

HSA-immobilized rectangular capillaries were prepared by dispensing 0.5 mL of 10 µg/mL HSA solutions into DMOAP-coated rectangular capillaries and kept at room temperature for 30 mins. After that, the inner surface of the capillaries was rinsed with copious amounts of DI water and dried under a stream of nitrogen. For the preparation of anti-HSA-immobilized rectangular capillaries, DMOAP-coated rectangular capillaries were fully loaded with 0.0005% PEI solutions for 1 h to generate amine function groups on the surface. Then, 0.5 mL of 1 µg/mL anti-HSA solutions was dispensed into the rectangular capillaries and kept at room temperature for 30 min. After that, the inner surface of the capillaries was rinsed with copious amounts of DI water and dried under a stream of nitrogen. Here, anti-HSA was oxidized to generate an aldehyde group on its Fc chain, which allows anti-HSA to form covalent bonding with the amine-functionalized surfaces. The detail procedures to prepare oxidized anti-HSA can be found in previous literature [15].

2.4 Preparation of artificial urine

Artificial urine was prepared according to the recipe that the aqueous solution contains 3.5 mM calcium chloride, 3 mM magnesium chloride, 72.1 mM sodium chloride, 18.7 mM monopotassium phosphate, 19.3 mM potassium chloride, 17.2 mM ammonium chloride and 41.6 mM urea. Then, the pH value of artificial urine was adjusted to 5.7 using hydrochloric acid.

2.5 LC-based immunoassay

For anti-HSA detection, different concentrations of anti-HSA were prepared in 0.6 mL centrifuge tubes by using $1 \times$ PBS buffer solution. The HSA-immobilized rectangular capillaries were then dipped into the anti-HSA solutions from one side and kept at room temperature for 2 h. After that, the capillaries were rinsed with copious amounts of buffer solution to remove the non-specifically adsorbed anti-HSA and dried under a stream of nitrogen. LC was drawn into the capillaries through capillary force. The optical appearance of the rectangular capillaries was observed by using a polarizing optical microscope (Leica, Germany) in transmission mode. Each image was captured by a digital camera mounted on the microscope using an exposure time of 1/80 s. To observe the capillaries using a smartphone, the capillaries were placed in between two pieces of crossed polarizers. Then the capillaries together with the polarizers were put on the screen of a smartphone of which the white backlight was turned on. For HSA detection, the experimental procedures were similar to that of anti-HSA detection. Instead, different concentrations of HSA solutions were prepared while anti-HSA-immobilized rectangular capillaries were used.

3. Results and discussion

3.1 Effect of DMOAP-coating on the optical image of LC inside the rectangular capillaries

To provide constant optical image as background signal for the LC-based immunoassay, the orientation of LC inside the rectangular capillaries should be well-controlled. For this reason, we studied how the surface coating inside the rectangular capillaries affects the optical image of LC. Figure 1(a) showed that the optical image of LC was bright inside the capillaries without DMOAP-coating. Specifically, the image of LC in the rectangular capillaries showed gray color, which was different from the colourful image of LC in the cell fabricated by two pieces of glasses. This observation can be explained different thickness of the LC layer in rectangular capillaries and in between two pieces of glasses [16,17]. The thickness of LC film in conventional LC cells was 3~10 μm , and the relationship between interference color and retardation of LC can be illustrated by using the Michel-Levy chart. In contrast, the thickness of LC film in the rectangular capillaries was 100 μm , which is much thicker than that in the LC cell and beyond the illustration of the Michel-Levy chart. In this condition, LCs in the capillary aligned randomly and the birefringence property of LCs was lost. Therefore, the LC images showed gray color. On the other hand, the optical image of LC was dark inside the capillaries with DMOAP-coating, suggesting the homeotropic orientation of LC on the glass substrate [Fig. 1(b)]. Previous studies demonstrated that the immunobinding on the DMOAP-modified glass substrate caused homeotropic-to-planar transition of the orientation of LC on the surface [10,11,18]. Therefore, we selected DMOAP-modified rectangular capillaries as the initial substrates for further investigations on the LC-based immunoassays.

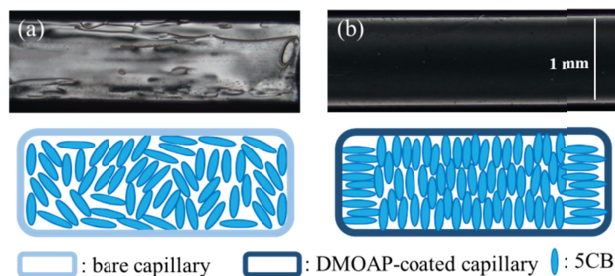


Fig. 1. Polarized images of (a) bare rectangular capillaries and (b) rectangular capillaries (top view) with DMOAP-coating on the inner surface. The schematic at the bottom illustrated the orientation of LC in the capillaries (cross section). It shows that the orientation of LC is homeotropic in DMOAP-coated capillaries and a dark LC image was shown.

3.2 Immobilization of HSA inside the rectangular capillaries

To test the feasibility of LC-based immunoassay using rectangular capillaries as platform, we immobilized human serum albumin (HSA) on the inner surface of rectangular capillaries substrate as the probe to capture anti-human serum albumin (anti-HSA) in the aqueous solution. To examine how the immobilized HSA disrupts the orientation of LCs inside the rectangular capillaries, we dispensed the solutions containing 100, 50, 40, 30, and 0 $\mu\text{g}/\text{mL}$ of HSA into the capillaries through capillary forces. After immobilization, the capillaries were rinsed by buffer solutions to remove the non-specifically adsorbed HSA. Figure 2 shows the optical images of these capillaries dispensed with 5CB. The results showed that bright LC image appeared when concentrations of HSA are 40 $\mu\text{g}/\text{mL}$ or above [Fig. 2(a)–(c)]. For the capillaries with the concentrations of HSA lower than 30 $\mu\text{g}/\text{mL}$, LC image remained dark [Fig. 2(d)]. Furthermore, when we dispensed the solution containing 30 $\mu\text{g}/\text{mL}$ of FITC-labeled HSA into the capillaries, fluorescent image was observed [Fig. 2(e)–(h)]. This result suggests that HSA was immobilized onto the inner surface of rectangular capillaries. When the density of surface-immobilized HSA was up to a critical value, HSA disrupted the

original orientation of LCs, i.e. homeotropic orientation. Therefore, a dark-to-bright transition of LC image in the capillaries was observed. Because a dark image of LC is required as the background signal of the LC-based immunoassay, we choose the capillaries immobilized with 30 $\mu\text{g}/\text{mL}$ of HSA in the following experiments to expect the optical transition of LC in the presence of anti-HSA in the capillaries.

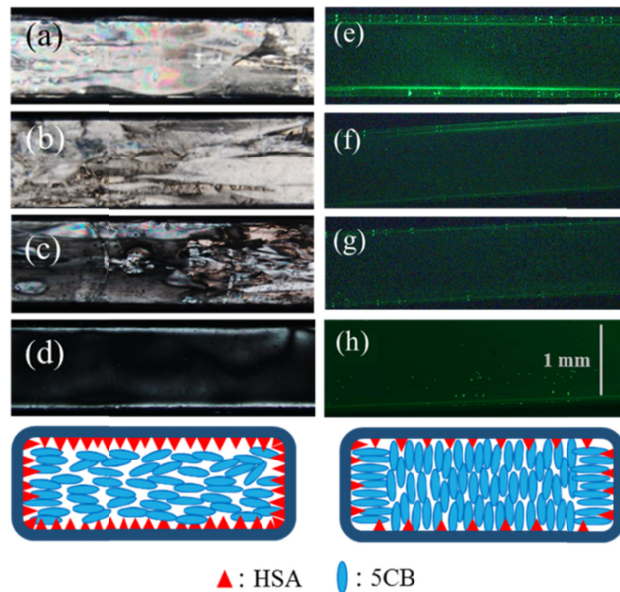


Fig. 2. Polarized images of rectangular capillaries (top view) immobilized with (a) 100, (b) 50, (c) 40, and (d) 30 $\mu\text{g}/\text{mL}$ of HSA. In (e-h), the capillary was immobilized with (e) 100, (f) 50, (g) 40 and (h) 30 $\mu\text{g}/\text{mL}$ of FITC-labeled HSA. The schematic at the bottom illustrated two different orientations of LC in the capillaries (cross section). It shows that LC image was bright in capillaries when the concentration of HSA was 40 $\mu\text{g}/\text{mL}$ or above.

3.3 Detection of anti-HSA and HSA

With the HSA-immobilized rectangular capillaries, our next step is to study how the optical signal of LC-based immunoassay response to the immunobinding of anti-HSA inside the capillaries. To achieve this goal, we dispensed 50 $\mu\text{g}/\text{mL}$ of anti-HSA solution into the HSA-immobilized capillaries. After immunobinding, the capillaries were rinsed by buffer solutions then dispensed with 5CB. As shown in Fig. 3(a), we found that the LC image of the capillaries with immobilized HSA, which were originally dark in the absence of anti-HSA, turned bright. This result suggests that anti-HSA could bind to HSA on the surface to form the immunocomplex with larger size, which disrupted the orientation of LC and resulted in a dark-to-bright transition of the LC image. As a control experiment, we dispensed 0 $\mu\text{g}/\text{mL}$ of anti-HSA solution into the HSA-immobilized capillaries. The result in Fig. 3(b) showed that the LC images were dark, which means the HSA/anti-HSA immunocomplex was not formed on the surface and therefore the orientation of LC was not disrupted. Based on these results, the presence of anti-HSA in the solution can be determined through the dark-to-bright transition of LC image in the rectangular capillary. The activity of the HSA-immobilized rectangular capillaries for anti-HSA detection could maintain for one month when the capillaries were stored under vacuum environment. On the other hand, we also studied the feasibility of this system to detect HSA, which is an important biomarker in urine for renal failure related diseases. In this case, we dispensed 75 $\mu\text{g}/\text{mL}$ and 0 $\mu\text{g}/\text{mL}$ of HSA solutions into the anti-HSA-immobilized capillaries, respectively. The results in Fig. 4 showed that the LC image of the capillaries was bright in the presence of HSA, while it was dark in the

absence of HSA. These results demonstrated that the presence of HSA in the solution can also be determined through the dark-to-bright transition of LC image in the rectangular capillary, which illustrated the diversity of the LC-based immunoassay.

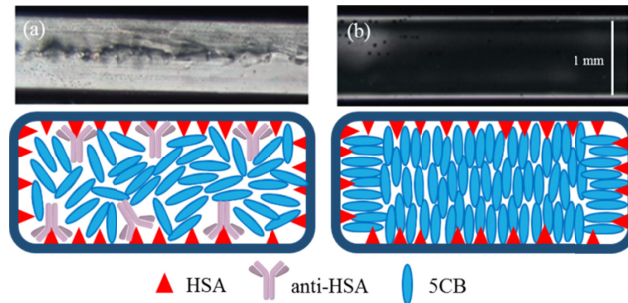


Fig. 3. Polarized images of rectangular capillaries (top view) immobilized with 30 $\mu\text{g/mL}$ of HSA dispensed with (a) 50 $\mu\text{g/mL}$ of anti-HSA and (b) 0 $\mu\text{g/mL}$ of anti-HSA. It shows that LC image turned bright in capillaries when anti-HSA bound to HSA in the capillaries.

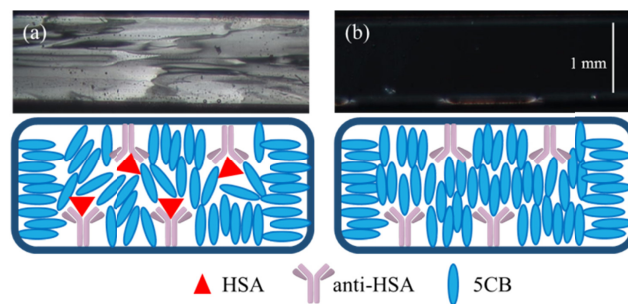


Fig. 4. Polarized images of rectangular capillaries (top view) immobilized with 1 $\mu\text{g/mL}$ of anti-HSA dispensed with (a) 75 $\mu\text{g/mL}$ of HSA and (b) 0 $\mu\text{g/mL}$ of HSA. It shows that LC image turned bright in capillaries when HSA bound to anti-HSA in the capillaries.

3.4 Quantification of the LC-based immunoassays using rectangular capillaries

To provide quantitative information of the LC-based immunoassays using rectangular capillaries as platform, we dipped the HSA-immobilized capillaries into the solutions containing different concentrations of anti-HSA to allow the solutions to dispense into the capillaries through capillary action. We anticipated that the inner surface of rectangular capillaries should become more hydrophilic when anti-HSA bound to the HSA immobilized on the surface. Therefore, when anti-HSA solutions are dispensed into the capillaries through capillary action, the liquid level of the capillaries would increase as the concentration of anti-HSA increases. Because bright LC images in the rectangular capillary could only appear at the region where the surface-immobilized HSA were in contact with anti-HSA, the length of the bright LC image in the rectangular capillary should relate to the concentration of anti-HSA solutions. The results in Fig. 5(a) showed that the LC images in the rectangular capillary were bright when the concentration of anti-HSA was 1 $\mu\text{g/mL}$ and above. When the concentration of anti-HSA was below 1 $\mu\text{g/mL}$, the solution cannot be dispensed into the capillary through capillary action such that the LC image of the capillary was totally dark. Based on these results, we can set the limit of detection (LOD) of this system for anti-HSA is 1 $\mu\text{g/mL}$. In addition, the plot in Fig. 5(b) shows that the length of the bright LC image in the rectangular capillary increased as the concentration of anti-HSA increased. The correlation coefficient for the linear line plotted with the length of the bright LC image as a function of the concentration of anti-HSA from 1 $\mu\text{g/mL}$ to 40 $\mu\text{g/mL}$ is 0.972. In contrast, this correlation coefficient decreased to 0.959 when the concentration of anti-HSA was ranging

from 1 $\mu\text{g}/\text{mL}$ to 60 $\mu\text{g}/\text{mL}$. Apparently, the deviation from linearity was occurred at high anti-HSA concentrations. At high anti-HSA concentrations, the liquid level of the capillaries approached to the open end of the capillary. Therefore, the deviation from linearity of this assay can be attributed to the offset of capillary force by the atmospheric pressure when the liquid level in the capillary was close to the open end of capillary. Based on this observation, it is expected that the linear range of this assay can be extended by using a longer rectangular capillary. In addition, the time required for the LCs to fill up in DMOAP-coated capillaries immobilized with HSA/anti-HSA immunocomplex was around 4 min, which is shorter than that in bare capillaries (~ 17 min) and is longer than that in DMOAP-coated capillaries. Apparently, the adsorption kinetics of 5CB is affected by the surface modifications of capillaries. We found that the time required for 5CB to fill up in the capillaries was shorter when the inner surface of capillaries was more hydrophobic. Because 5CB is hydrophobic, this phenomenon can be explained by the enhanced hydrophobic interactions between 5CB and DMOAP-coated surface. In previous study, LC-based immunoassay has been developed by using microfluidics as the detection platform [19]. In their results, proteins were adsorbed in the microfluidics in gradient fashion, as the LCs showed different colors in the microfluidics. In contrast, gradient adsorption of anti-HSA was not observed in the rectangular capillaries. This phenomenon can be explained by the dip coating approach of anti-HSA. In our experiments, the capillaries were dipped into 200 μL of anti-HSA solutions and kept for 2 h for immunobinding. However, the volume required to fill the capillaries was only 50 μL , which means anti-HSA in the solution would keep going into the capillaries in 2 h and the adsorption of anti-HSA in capillaries reached equilibrium at the end of the experiments.

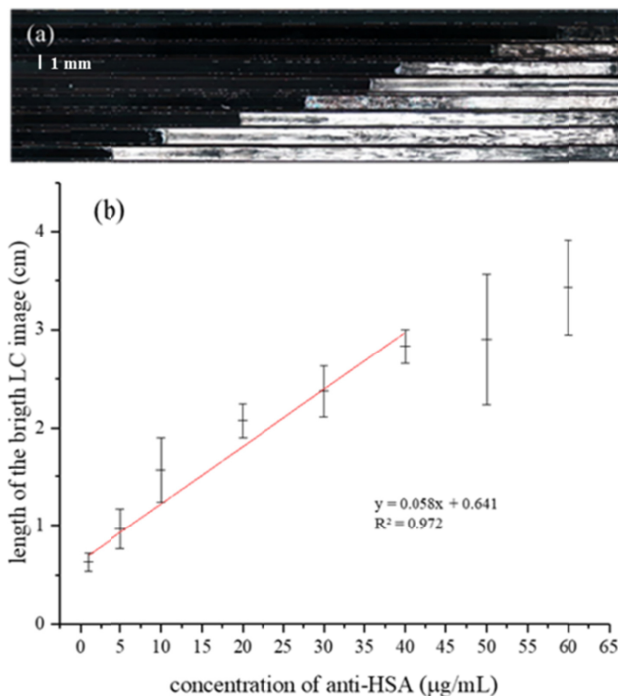


Fig. 5. (a) Polarized images of rectangular capillaries (top view) immobilized with 10 $\mu\text{g}/\text{mL}$ of HSA then dispensed with 0, 1, 5, 10, 20, 30, 40, 50 and 60 $\mu\text{g}/\text{mL}$ of anti-HSA (from top to bottom) through capillary action. (b) Correlations between the brightness length of the capillaries and the concentration of anti-HSA. The error bars indicate the standard deviation of the measurements of five repeated experiments for each assay. It shows that brightness length of the capillaries increased as the concentration of anti-HSA.

3.5 Detection of anti-HSA in artificial urine

To test the practicability of the LC-based immunoassays using rectangular capillaries as sensing platform, we tried to detect the presence of anti-HSA in artificial urine samples because there are many important biomarkers for diseases diagnosis in human urines. The experiments were performed by spiking different concentrations of anti-HSA in artificial urine solutions. Figure 6(a) showed that the LC images in the rectangular capillary were bright when the concentration of anti-HSA was 1 $\mu\text{g}/\text{mL}$ and above, while it was dark when the concentration of anti-HSA was 1 $\mu\text{g}/\text{mL}$ and below. Therefore, the LOD of the LC-based immunoassays using rectangular capillaries as platform for anti-HSA detection in artificial urine was 1 $\mu\text{g}/\text{mL}$, which is the same as that in buffer solutions. In terms of quantitative information, the correlation coefficient for the linear line plotted with the length of the bright LC image as a function of the concentration of anti-HSA from 1 $\mu\text{g}/\text{mL}$ to 40 $\mu\text{g}/\text{mL}$ is 0.900, as shown in Fig. 6(b). We found that the average length of the bright LC image in the rectangular capillary was longer in urine samples than in buffer samples. This result can be explained by the high concentration of urea in urine. Urea is an amine-rich molecule which significantly increased the interactions between the protein-immobilized surface and aqueous solutions such that resulted in a higher water level of capillary through capillary action. Because the length of capillary was fixed, longer length of the bright LC image in the rectangular capillary would make the linear range of the LC-based immunoassay smaller. Nevertheless, our results demonstrated the quantitative detection of anti-HSA in urine by using the LC-based immunoassays using rectangular capillaries as platform, which shows its potential applicability for disease diagnosis.

Furthermore, we investigated the specificity and interference effect of LC-based immunoassay because an ideal immunoassay should not be interfered with non-specific binding which leads to false-positive results. To achieve this goal, we performed another three experiments by using the artificial urine solutions containing 20 $\mu\text{g}/\text{mL}$ HSA, 20 $\mu\text{g}/\text{mL}$ IgG, and 20 $\mu\text{g}/\text{mL}$ IgG together with 20 $\mu\text{g}/\text{mL}$ anti-HSA, respectively. The results in Fig. 6(c) showed that the LC images in the rectangular capillary were dark when the solutions contained HSA or IgG, which means HSA or IgG would not bind to surface-immobilized HSA to disrupt the orientation of LC. On the other hand, Fig. 6(c) showed that the LC image in the rectangular capillary was bright when the solutions contained IgG together with anti-HSA. The length of the bright LC image in the rectangular capillary was 2.92 cm, which is comparable to the result using the artificial urine solutions containing only anti-HSA (3.02 ± 0.1 cm). The above results, when combined, led us to conclude that the detection of anti-HSA by using LC-based immunoassay was specific; it was not interfered by other common proteins in human urines such as HSA and IgG.

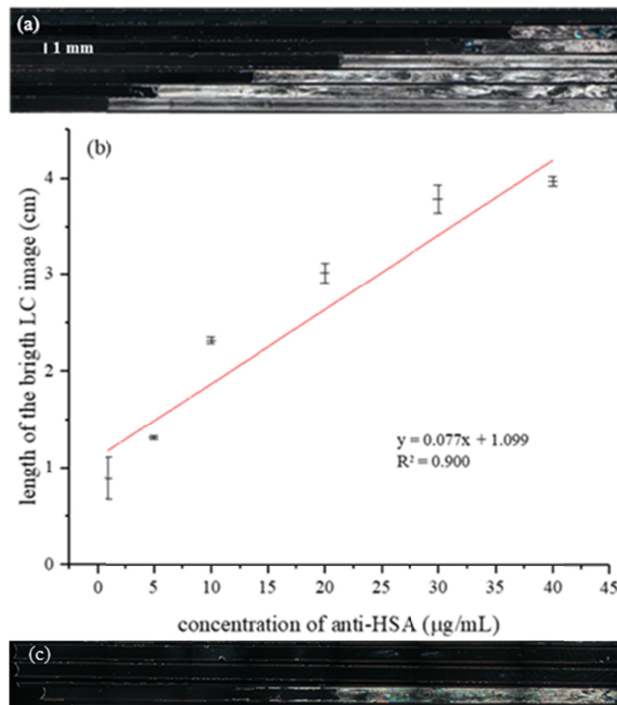


Fig. 6. (a) Polarized images of rectangular capillaries (top view) immobilized with 10 $\mu\text{g/mL}$ of HSA then dispensed with 0, 1, 5, 10, 20, 30 and 40 $\mu\text{g/mL}$ of anti-HSA (from top to bottom) in artificial urine through capillary action. (b) Correlations between the brightness length of the capillaries and the concentration of anti-HSA. The error bars indicate the standard deviation of the measurements of five repeated experiments for each assay. (c) Polarized images of rectangular capillaries (top view) immobilized with 10 $\mu\text{g/mL}$ of HSA then dispensed with 20 $\mu\text{g/mL}$ of HSA, 20 $\mu\text{g/mL}$ of IgG and 20 $\mu\text{g/mL}$ of IgG together with 20 $\mu\text{g/mL}$ of anti-HSA (from top to bottom) in artificial urine through capillary action. It shows that the LC-based immunoassays can be applied in urine samples for anti-HSA detection, and it was not interfered with HSA and IgG.

3.6 Recording the signal of LC-based immunoassay by using smartphone

Most of previous studies on LC-based sensing platforms applied polarizing optical microscopy (POM) to record the optical signal of LCs, which limits their application for portable detection. Because the signals of LC-based immunoassay can be observed through naked-eye under ambient light, it is anticipated that the LC signals can also be recorded by using a smartphone. In this case, the signal recording system for LC-based immunoassays is portable which makes them more suitable for on-site applications. To explore whether the signals for the LC-based immunoassays using rectangular capillaries can be recorded by using a smartphone, we prepared three rectangular capillaries which were dispensed with 0, 10 and 100 $\mu\text{g/mL}$ of anti-HSA in artificial urines, respectively. Then, they were placed in between two pieces of cross-polarizers. The capillaries together with cross-polarizers were put on the screen of a smartphone with white lights, followed by taking the photos of rectangular capillaries using another smartphone. Figure 7 showed that the bright and dark LC images of LC-based immunoassay were clear to human naked eye. In addition, the length of the bright LC image can be easily differentiated when a scale bar was integrated on the observing system. Specifically, the bright LC image in the rectangular capillary for 0, 10 and 100 $\mu\text{g/mL}$ of anti-HSA was 0, 1.5 and 4.5 cm, respectively, which are in accordance with the linear correlation shown in Fig. 6(b). These results demonstrated that the quantitative information of the LC-based immunoassays using rectangular capillaries as sensing platform is readily understandable to the general users.



Fig. 7. The image of LC-based immunoassay captured by a smartphone. It shows that the LC image was clear, and the length of the bright LC image can be easily differentiated with an integrated scale bar.

4. Conclusions

In conclusions, we developed the LC-based immunoassays for anti-HSA detection by using rectangular capillaries as the sensing platform. The detection mechanism was based on the specific immunobinding occurred on the inner surface of capillary, which disrupted the original orientation of LC and led to a dark-to-bright transition of the LC images. By using this assay, the LOD for anti-HSA is $1 \mu\text{g/mL}$ with the linear range from $1 \mu\text{g/mL}$ to $40 \mu\text{g/mL}$. We also demonstrated the feasibility of the assay to detect anti-HSA in urine samples with good specificity. The signals of the assay can be recorded by using a smartphone as the detector. In contrast to previous LC-based sensors that applied the gray scale value of the LC images for quantitative analysis, the signals of the LC-based immunoassays using rectangular capillaries as sensing platform were quantified by measuring the length of the LC image in the capillaries that is readily understandable to the general users. Because the post-fabrication of LC cell was waived by using rectangular capillaries to develop LC-based immunoassays, it is more simple and convenient for users to handle the immunoassay and could be more suitable for portable and on-site applications.

Funding

Ministry of Science and Technology, Taiwan (MOST 107-2113-M-032-003-)

Disclosures

The authors declare that there are no conflicts of interest related to this article.

References

1. C. M. Cheng, A. W. Martinez, J. Gong, C. R. Mace, S. T. Phillips, E. Carrilho, K. A. Mirica, and G. M. Whitesides, "Paper-based ELISA," *Angew. Chem. Int. Ed. Engl.* **49**(28), 4771–4774 (2010).
2. A. Ambrosi, F. Airò, and A. Merkoçi, "Enhanced gold nanoparticle based ELISA for a breast cancer biomarker," *Anal. Chem.* **82**(3), 1151–1156 (2010).
3. J. Liang, C. Yao, X. Li, Z. Wu, C. Huang, Q. Fu, C. Lan, D. Cao, and Y. Tang, "Silver nanoprism etching-based plasmonic ELISA for the high sensitive detection of prostate-specific antigen," *Biosens. Bioelectron.* **69**, 128–134 (2015).
4. Y. Wu, L. Zeng, Y. Xiong, Y. Leng, H. Wang, and Y. Xiong, "Fluorescence ELISA based on glucose oxidase-mediated fluorescence quenching of quantum dots for highly sensitive detection of Hepatitis B," *Talanta* **181**, 258–264 (2018).
5. K. Kitamura, K. Matsuda, M. Ide, T. Tokunaga, and M. Honda, "A fluorescence sandwich ELISA for detecting soluble and cell-associated human interleukin-2," *J. Immunol. Methods* **121**(2), 281–288 (1989).
6. S. K. Arya and P. Estrela, "Electrochemical ELISA-based platform for bladder cancer protein biomarker detection in urine," *Biosens. Bioelectron.* **117**, 620–627 (2018).
7. A. C. Glavan, D. C. Christodouleas, B. Mosadegh, H. D. Yu, B. S. Smith, J. Lessing, M. T. Fernández-Abedul, and G. M. Whitesides, "Folding analytical devices for electrochemical ELISA in hydrophobic R(H) paper," *Anal. Chem.* **86**(24), 11999–12007 (2014).

8. H. W. Su, M. J. Lee, and W. Lee, "Surface modification of alignment layer by ultraviolet irradiation to dramatically improve the detection limit of liquid-crystal-based immunoassay for the cancer biomarker CA125," *J. Biomed. Opt.* **20**(5), 57004 (2015).
9. W. H. Ho and C. H. Chen, "Liquid crystal-based immunoassay for detecting human serum albumin," *Res. Chem. Intermed.* **40**(6), 2229–2236 (2014).
10. C. H. Chen and K. L. Yang, "Liquid crystal-based immunoassays for detecting hepatitis B antibody," *Anal. Biochem.* **421**(1), 321–323 (2012).
11. C. Y. Xue, S. A. Khan, and K. L. Yang, "Exploring optical properties of liquid crystals for developing label-free and high-throughput microfluidic immunoassays," *Adv. Mater.* **21**(2), 198–202 (2009).
12. A. Shirai, T. G. Henares, K. Sueyoshi, T. Endo, and H. Hisamoto, "Fast and single-step immunoassay based on fluorescence quenching within a square glass capillary immobilizing graphene oxide-antibody conjugate and fluorescently labelled antibody," *Analyst (Lond.)* **141**(11), 3389–3394 (2016).
13. M. Khan and S. Y. Park, "Liquid crystal-based biosensor with backscattering interferometry: A quantitative approach," *Biosens. Bioelectron.* **87**, 976–983 (2017).
14. H. J. Kim and C. H. Jang, "Micro-capillary sensor for imaging trypsin activity using confined nematic liquid crystals," *J. Mol. Liq.* **222**, 596–600 (2016).
15. W. H. Ho and C. H. Chen, "Liquid crystal-based immunoassay for detecting human serum albumin," *Res. Chem. Intermed.* **40**(6), 2229–2236 (2014).
16. C. H. Chen and K. L. Yang, "Detection and quantification of DNA adsorbed on solid surfaces by using liquid crystals," *Langmuir* **26**(3), 1427–1430 (2010).
17. C. Y. Xue and K. L. Yang, "Dark-to-bright optical responses of liquid crystals supported on solid surfaces decorated with proteins," *Langmuir* **24**(2), 563–567 (2008).
18. W. Zhang, W. T. Ang, C. Y. Xue, and K. L. Yang, "Minimizing nonspecific protein adsorption in liquid crystal immunoassays by using surfactants," *ACS Appl. Mater. Interfaces* **3**(9), 3496–3500 (2011).
19. C. Y. Xue, S. A. Khan, and K. L. Yang, "Exploring optical properties of liquid crystals for developing label-free and high-throughput microfluidic immunoassays," *Adv. Mater.* **21**(2), 198–202 (2009).